European Journal of Pharmaceutics and Biopharmaceutics 73 (2009) 95–101

Contents lists available at ScienceDirect

European Journal of Pharmaceutics and Biopharmaceutics

journal homepage: www.elsevier.com/locate/ejpb

Research paper

Physicochemical and pharmacological characterization of novel vasoactive intestinal peptide derivatives with improved stability

Satomi Onoue [a,*], Shingen Misaka [a], Yuki Ohmori [a], Hideyuki Sato [a], Takahiro Mizumoto [c], Mariko Hirose [c], Sumiko Iwasa [b], Takehiko Yajima [b], Shizuo Yamada [a]

[a] Department of Pharmacokinetics and Pharmacodynamics, University of Shizuoka, Shizuoka, Japan
[b] Department of Analytical Chemistry, Toho University, Chiba, Japan
[c] Department of Product Development, ILS Inc., Ibaraki, Japan

ARTICLE INFO

Article history:
Received 27 June 2008
Accepted in revised form 25 May 2009
Available online 28 May 2009

Keywords:
VIP
Stability
Receptor binding
Neurite outgrowth
UPLC–MS

ABSTRACT

Previously, [$R^{15,20,21}$, L^{17}]-VIP-GRR (IK312532), a long-acting VIP derivative, was proposed as potential drug candidate for the treatment of asthma/COPD. The present work is aimed to elucidate solution-state stability of IK312532 and to develop further stabilized derivative with equipotent or higher biological functions. A stability study on IK312532 was carried out in solution state, and degradation mechanism was deduced by UPLC–MS and amino acid analyses. Three novel VIP derivatives were designed and chemically synthesized on the basis of stability data, being subjected to physicochemical and pharmacological characterization. Solution-state stability studies revealed the gradual degradation of IK312532, following pseudo-first-order kinetics. Chemical modification of IK312532, mainly position at 24, resulted in marked improvement of stability, although the chemical modification had no influence on the secondary structure, receptor binding, and activation of adenylate cyclase in rat lung cells. Novel derivatives also exhibited more potent neurite outgrowth in rat pheochromocytoma PC12 cells when compared to VIP and IK312532, possibly due to improved stability. Deamination of Asn at position 24 might be responsible for degradation of VIP derivative, and stability and chemical modification studies led us to the successful development of novel VIP derivatives with higher stability and biological functions.

1. Introduction

Vasoactive intestinal peptide (VIP) [1], an octacosapeptide, is a member of glucagon/secretin superfamily [2]. VIP and its receptor are widely distributed in the body, such as in the heart, lung, digestive and genitourinary tract, eye, skin, ovaries, and thyroid gland [3]. VIP is one of the major peptide transmitters in the central and peripheral nervous systems, being involved in a wide range of biological functions in organisms, including metabolic processes, exocrine and endocrine secretions, cell differentiation, relaxation of smooth muscle [4], secretion of regulatory hormones [5], and regulation of immune response [6]. On the basis of its numerous biological actions, VIP has been considered to be a potential candidate for pharmaceutical agents for several diseases, including diabetes [7], asthma [4], impotence [8], and rheumatism [9].

While the pharmacological potency of a peptide itself may be of general importance, chemical and physical stability is also a critical factor in the drug design of peptide for overall therapeutic success. In particular, the rapid degradation of VIP after systemic administration is part of the reason for the limitation of its clinical applications. Therefore, for the clinical application of VIP as a therapeutic agent, a metabolically stable analogue of VIP needs to be developed, and many structure–activity relationship (SAR) studies focusing on VIP stabilization have been carried out [10,11]. Our group previously conducted chemical modification studies to investigate the SARs of VIP by using synthetic VIP analogues. The replacement of Lys residue at the positions 15, 20, and 21 by Arg, and Met at position 17 by Leu ([$R^{15,20,21}$, L^{17}]-VIP) in VIP resulted in a significant improvement in metabolic stability [11]. In addition, C-terminally extended VIP derivative, IK312532, [$R^{15,20,21}$, L^{17}]-VIP-GRR, exhibited much higher biological activity than natural VIP *in vitro* and *in vivo* [12]. Interestingly, IK312532 showed a higher stability against enzymatic digestion and even higher biological activity, including relaxant effect and protective effect against the cytotoxicity of CSE and deactivation of CSE-evoked caspase-3, compared to VIP [13,14]. By combining the clinical advantages of bronchodilation and protection of the alveolar wall,

* Corresponding author. Department of Pharmacokinetics and Pharmacodynamics and Global Center of Excellence (COE) Program, School of Pharmaceutical Sciences, University of Shizuoka, 52-1 Yada, Suruga-ku, Shizuoka 422-8526, Japan. Tel.: +81 54 264 5633; fax: +81 54 264 5635.
E-mail address: onoue@u-shizuoka-ken.ac.jp (S. Onoue).

0939-6411/$ - see front matter © 2009 Elsevier B.V. All rights reserved.
doi:10.1016/j.ejpb.2009.05.013

stabilized VIP derivatives could provide a novel and more effective pharmacotherapy for the treatment of asthma and COPD [11].

In the present investigation, further improvement of IK312532 was attempted by some chemical modifications. Stability of IK312532 in solution state was assessed at several conditions, and the structures of main degradants were deduced by amino acid analysis of isolated substances and UPLC–MS experiments. Novel VIP derivatives were developed on the basis of stability data on IK312532. Physicochemical and pharmacological properties of newly synthesized VIP derivatives were characterized by solution-state stability studies using UPLC–MS, circular dichroism (CD), receptor-binding assay, activation of adenylate cyclase, and neurite outgrowth stimulation in PC12 cells.

2. Materials and methods

2.1. Peptides syntheses

VIP and derivatives (Table 1) were chemically synthesized by the solid-phase strategy employing optimal side-chain protection as reported previously [15]. Peptides were removed from the resin by HF treatment, and the cleaved products were purified using column chromatography over Chromatorex ODS (Fuji Silysia, Aichi, Japan) with CH_3CN–H_2O system mobile phase. The purity (>98%) was checked by reverse-phase HPLC using a TSK-gel ODS-120T column (Tosoh, Tokyo, Japan). Their molecular weights were confirmed on a matrix-assisted laser desorption ionization time of flight mass spectrometer (Kratos, Manchester, UK).

2.2. Solution-state stability study

Solutions of peptide (0.1 mg/mL) dissolved in 20 mM phosphate buffer (pH 7.4) in 5 mL glass vial were stored at 4, 40, or 55 °C for various periods. At selected times, the solutions were directly subjected to UPLC analysis to monitor the degradation of tested samples. All analyses were performed on Waters Acquity UPLC /MS system (Waters, Milford, MA), which include the binary solvent manager, sampler manager, column compartment, Acquity TUV detector with the detection wavelength of 254 nm, and single quadrupole mass detector (mass range: m/z 300–2000), connected with Waters MassLynx software. The mass spectrometer instrument was operated in positive electrospray ionization mode using cone voltages of 50 mV. The source and desolvation temperatures were set at 120 and 400 °C, respectively. An Acquity UPLC BEH C18 column (particle size: 1.7 μm, column size: Φ2.1 × 50 mm; Waters), also from Waters, was used. Column temperature was maintained at 40 °C. The mobile phase consisted of 0.1% trifluoroacetic acid (TFA)–acetonitrile 75:25 (v/v) with flow rate of 0.25 mL/min.

2.3. Amino acid analysis

Each purified peptide (0.25 mg) was vacuum dried in amino acid analysis vial and subsequently placed in hydrolysis reaction vial containing 6 M HCl containing 1% phenol. To remove oxygen, the reaction vial was degassed by vacuum and purged with nitrogen in a Waters Pico-Tag Workstation (Waters) at least three times. Each sample was placed under vacuum and then gas-phase hydrolyzed at 110 °C for 24 h. After acid hydrolysis, each sample was vacuum dried and then solubilized in water. Each solution was filtered through a 0.45 μm membrane filter and analyzed in amino acid analyzer Hitachi L8500 (Hitachi, Tokyo, Japan) according to the manufacturer's protocol. The analyses for determination of amino acid compositions were performed in triplicate.

2.4. Circular dichroism

For circular dichroism (CD) analysis, each peptide was dissolved in either 20 mM Tris–HCl (pH 7.4) or 50% methanol (MeOH)/20 mM Tris–HCl buffer. CD spectra were baseline corrected and smoothed using the algorithm provided by the manufacturer, and they were recorded at room temperature in a Jasco model J-720 spectropolarimeter (Jasco, Tokyo, Japan) with a cell path length of 10 mm. Each sample was scanned five times in the wavelength range of 200–400 nm (scan speed: 10 nm/min; sensitivity: 20 mdeg). Ellipticity was calculated as mean residue ellipticity [θ] (degrees $cm^2\ dmol^{-1}$). The secondary structures of synthetic peptides were evaluated from CD spectra using four independent methods established by Chen and Yang [16], Greenfield and Fasman [17], and k2d software for analyzing the CD spectra [18].

2.5. Cell cultures

L2 cells, originally derived from type II pneumocytes of adult rat lung [19], were obtained from the American Type Culture Collection (Rockville, MD). L2 cells were cultured in Dulbecco's modified Eagle's medium (DMEM; Sigma) supplemented with 10% (v/v)

Table 1
Sequence of VIP and its derivatives.

	5 10 15 20 25 30	α-Helix (%)
VIP	H S D A V F T D N Y T R L R K Q M A V K K Y L N S I L N	63
Secondary structure	*Random coil* / ***α-Helix*** / *Random coil*	
[$R^{15,20,21}$, L^{17}]-VIP-GRR (IK312532)	– – – – – – – – – – – – – – – R – L – – R R – – – – – – – G R R	62
[$R^{15,20,21}$, L^{17}, $A^{24,25}$, des-N^{28}]-VIP-GRR (IK312548)	– – – – – – – – – – – – – – – R – L – – R R – – A A – – G R R	58
[E^{8}, $R^{15,20,21}$, L^{17}, $A^{24,25}$, des-N^{28}]-VIP-GRR (IK312550)	– – – – – – – E – – – – – – – R – L – – R R – – A A – – G R R	58
[$A^{8,24,25}$, $R^{15,20,21}$, L^{17}, des-N^{28}]-VIP-GRR (IK312551)	– – – – – – – A – – – – – – – R – L – – R R – – A A – – G R R	63

All peptides were synthesized by the solid-phase strategy employing optimal side-chain protection and amidated at their C-terminuses. Helical content was deduced by CD spectral analysis, according to the equation established by Greenfield and Fasman [17].

newborn calf serum (HS; Gibco-BRL, Grand Island, NY). The cultures were maintained in 5% CO_2 or 95% humidified air at 37 °C.

2.6. [^{125}I]VIP-binding assay

[^{125}I]VIP-binding assay was performed using the procedure described by Leroux et al. [20] with some modifications . L2 cells were added to ice-cold Hanks' balanced salt solution (HBSS, pH 7.35) and centrifuged at 1000 rpm for 5 min. The pellet was homogenized in ice-cold buffer (100 ml of HBSS, 1 mL of 1 M *N*-2-hydroxyethylpiperazine-*N*′-2-ethanesulfonic acid (HEPES), and 1 g of bovine serum albumin (BSA) at pH 7.35) with a Potter glass homogenizer. The homogenates prepared from L2 cells were incubated with [^{125}I]VIP (0.03–1.50 nM) in a total volume of 100 μL. Incubation was carried out for 3 h at 4 °C. The reaction was terminated by rapid filtration (Cell Harvester, Brandel Co., Gaithersburg, MD) through Whatman GF/C glass fiber filters presoaked in 0.5% polyethyleneimine solution for 1 h, and the filters were rinsed three times with 2 mL of ice-cold buffer. The tissue-bound radioactivity was determined in a *gamma*-counter. The specific binding of [^{125}I]VIP was determined experimentally from the difference between counts in the absence and presence of 3 μM unlabeled VIP. All assays were conducted in duplicate. Protein concentrations of cell lysates were measured by the method as described by Lowry et al. [21] with BSA as the standard.

2.7. Reverse Transcriptional PCR (RT-PCR) Amplification

The mRNA was isolated from PC12 cells using a commercially available kit (QuickPrep Micro mRNA Purification Kit; Amersham Pharmacia Biotech, Piscataway, NJ, USA), and the synthesis of the first-strand cDNA was performed using the Ready-To-Go T-Primed First-Strand Kit (Amersham Pharmacia Biotech). The RT reaction was also carried out in the absence of reverse transcriptase to ensure that the amplified material derived from RNA. The RT-PCR primers designed for the PACAP/VIP receptors (PAC1, VPAC1, and VPAC2) and the glucagon receptor [5] were as follows: 5′- and 3′-primers for PAC1 were 5′-TTTCA TCGGC ATCAT CATCA TCATC CTT-3′ (sense) and 5′-CCTTC CAGCT CCTCC ATTTC CTCTT-3′ (antisense), those for VPAC1 were 5′-GCCCC CATCC TCCTC TCCAT C-3′ (sense) and 5′-TCCGC CTGCA CCTCA CCATT G-3′ (antisense), and those for VPAC2 were 5′-ATGGA TAGCA ACTCG CCTTT CTTTA G-3′ (sense) and 5′-GGAAG GAACC AACAC ATAAC TCAAA CAG-3′ (antisense). The size of each PCR product was expected to 280 base pairs (bp) for the basic PAC1 receptor, 364 bp for a PAC1 receptor with a single cassette insert (hip, hop1, or hop2), 448 bp for a double insert (hiphop1 or hiphop2), 299 bp for VPAC1, and 325 bp for VPAC2. The PCR were performed in 25 μL containing 1.5 mM $MgCl_2$, 50 mM KCl, 10 mM Tris–HCl (pH 9.0), 200 μM of each deoxynucleoside triphosphate, 0.4 μM of the specific oligonucleotide primers, and 1.5 units of *Taq* DNA polymerase. After the initial denaturation at 94 °C for 3 min, 35 cycles of amplification (30 s denaturing step at 94 °C, 30 s annealing step at 66 °C (PAC1, VPAC1) or at 63 °C (VPAC2), and a 1 min extension step at 72 °C) were performed in a DNA Thermal Cycler (Perkin Elmer, Norwalk, CT, USA). The products of amplification were separated on a 2% agarose gel in 1 × Tris–acetic acid–EDTA buffer, stained with ethidium bromide (0.5 μg/mL), visualized under ultraviolet light, and photographed.

2.8. Measurement of extracellular cAMP

PC12 cells (10^5 cells/well) in 96-well collagen I-coated plates (Becton Dickinson Labware, Bedford, MA) were stimulated for 30 min with ligand in the serum-free medium. Supernatants were collected, and aliquots (100 μL) were assayed using a kit for the determination of cyclic AMP by enzyme immunoassay according to the manufacturer's instructions (Amersham Pharmacia Biotech, Piscataway, NJ).

2.9. Neurite outgrowth

PC12 cells were plated in 60-mm Falcon culture dishes coated with collagen type IV (Becton Dickinson Labware, Bedford, MA, USA) at a density of 2×10^5 cells in 4 ml of medium per dish. After incubation of PC12 cells for 24 h, each peptide was added into culture media. The medium supplemented with neuropeptide was changed every 24 h. The cells were fixed in neutral-buffered (pH 7.4) 10% formalin, rinsed in distilled water, and then stained with hematoxylin–eosin. Every 10–40 selected cells in more than 4 fields from two culture dishes were subjected to analysis of morphological change. The neurite outgrowth of the cells cultured with various concentrations of peptide or vehicle (control) was evaluated by counting the number of differentiated cells having neurite with a length of >50 μm. The measurement was performed on a Macintosh computer using the public domain program *NIH Image* (version 1.62).

2.10. Data analysis

For statistical comparisons, a one-way analysis of variance (ANOVA) with the pairwise comparison by Fisher's least significant difference procedure was used. A P value of less than 0.05 was considered significant for all analyses.

3. Results and discussion

3.1. Solution-state stability of VIP derivative

In solution-state stability studies on IK312532, gradual degradation of IK312532 was observed during storage at several conditions, and the decomposition of IK312532 in sodium phosphate buffer (pH 7.4) was plotted in a typical logarithm of percent remaining versus time (Fig. 1A). Linear relationships were observed for all conditions tested, and the correlation coefficients were found to be greater than 0.95. This indicated that the degradation of IK312532 in aqueous-buffered solutions followed apparent first-order degradation kinetics under the conditions studied. The slope of the plot represents the apparent first-order degradation rate constant at each temperature, and they were calculated to be 2.5×10^{-3}, 0.21, and 0.69, respectively, per day for 4, 40, and 55 °C. Thus, the degradation process of IK312532 was highly accelerated with the increase in temperatures.

According to UPLC–MS chromatograms of IK312532 stored at 40 °C for 1 week (Fig. 1B), IK312532 was readily decomposed in sodium phosphate buffer, yielding three main degradants A, B, and C. The m/z ratios of the peaks were determined using UPLC–MS, and the molecular mass of these degradants were found to be 3762 Da (Table 2), indicating the slight changes in molecular mass when compared to IK312532 (3761 Da). For further characterization and identification of these chemicals, each degradant was isolated with use of preparative HPLC and subjected to amino acid analysis (Table 2). On the basis of the results from amino acid analysis, all degradants and IK312532 show similar amino acid composition; however, both Asx and Glx residues were not fully elucidated. These findings, taken together with their molecular mass, suggest that the deamination of Asn or Gln residues occurred in sodium phosphate buffer. IK312532, as well as VIP, has several asparaginyl and glutaminyl peptide, and especially Asn-Ser, at positions 24 and 25, can easily convert into a succinyl peptide (Asu) following deamination of the Asn residue [11,22,23]. The Asu formation

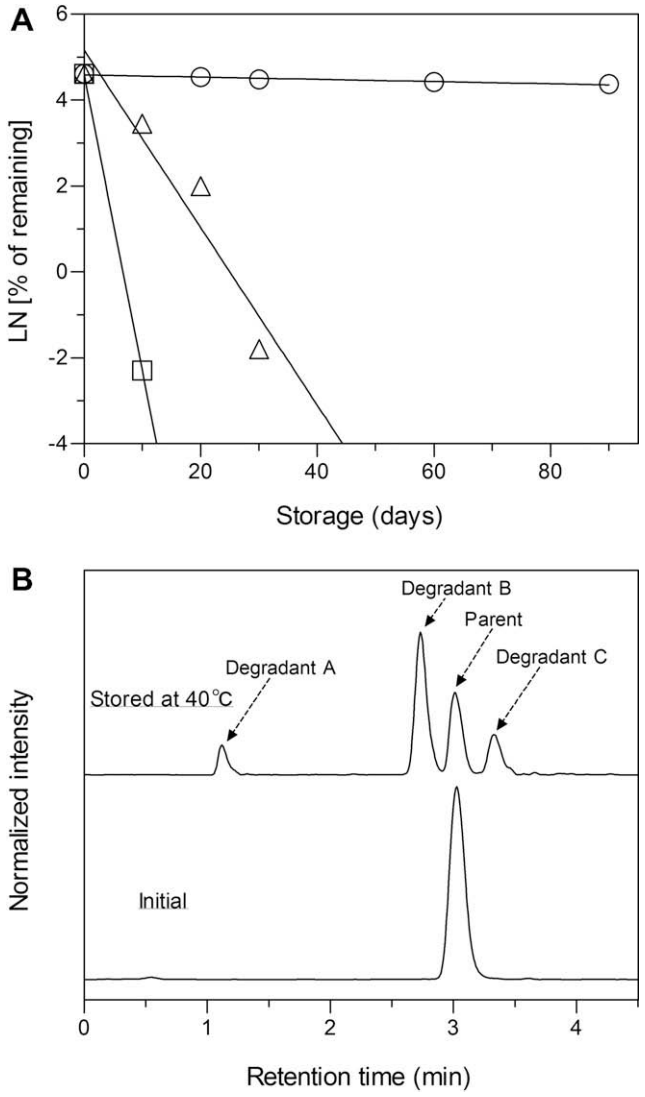

Fig. 1. Solution-state stability of IK312532. (A) Time-dependent degradation of IK312532. IK312532 (0.1 mg/mL) was dissolved in 20 mM sodium phosphate buffer (pH 7.4) and stored at 4, 40, and 55 °C for indicated periods. ○, stored at 4 °C; △, at 40 °C; and □, at 55 °C. Data represent mean of three experiments. (B) UPLC–MS chromatograms of degradation of IK312532. IK312532 (0.1 mg/mL) was stored at 40 °C for 1 week and then subjected to UPLC–MS analysis.

and its hydrolysis, leading to normal and isoaspartyl peptides, occurred in the pH range of 5–10, and the kinetic constants of these steps increase markedly at basic pH [22]. In this context, protection or replacement of Asn at position 24 by other bioequivalent residue was expected to be effective for improvement on chemical stability of VIP or its derivatives.

3.2. Design and structural characterization of novel VIP derivatives

Numerous conformational studies, including spectral and computational analyses, have characterized that VIP possesses two segments of secondary structures; a random coil structure in the N-terminal region containing ca 10 amino acid residues between positions 1 and 9, and a long α-helical structure in the C-terminal region stretching from position 10 to its C-terminus [24–26]. The α-helical structure of VIP, as well as other glucagon–secretin family peptides, was found to be essential for receptor binding [27], and disruption of helical structure led to marked decrease in biological activities. Thus, the replacement of Asn at position 24 might also affect α-helical structure in the C-terminus followed by decrease in biological activity, although the modification could improve chemical stability of VIP derivative. To maintain C-terminal helical structure, synthesis of chimeric peptides comprising VIP and PACAP was proposed, because PACAP exhibited as much as 68% sequential homology and high secondary structural similarity with VIP. Herein, novel VIP derivatives having Ala at positions 24 and 25 (Table 1) were designed and chemically synthesized, which correspond to residues at positions 24 and 25 in PACAP. Amino acid residue at position 8 was also substituted by other amino acid according to previous SAR information [28], and Asn at position 28 was deleted since the truncation did not affect receptor binding and smooth muscle relaxant activities in our previous work [27].

To clarify the influence of chemical modification on the secondary structure of VIP derivatives, the solution structures of novel VIP derivatives were deduced by CD spectral analysis with use of k2d software [18] (Fig. 2). The α-helical contents estimated by CD were variable depending on solvent systems such as pH and polarity; however, N-terminal random coil and C-terminal helical structures were maintained under any conditions tested (data not shown). According to the calculative method, VIP and its derivatives were estimated to contain ca 60% α-helical structure. The data suggest that the chemical modification did not affect the secondary structure of derivatives, and the chemicals were expected to maintain biological function of IK312532 with higher stability.

Table 2
UPLC/MS and amino acid analyses of IK312532 and its degradants.

	IK312532		Degradant A	Degradant B	Degradant C
Relative retention time	1.00		0.37	0.91	1.11
MS found (calculated)	3761		3762	3762	3762
Amino acid analysis	Expected	Measured	Measured	Measured	Measured
Ala	2	2.1	2.0	2.0	2.0
Arg	7	6.8	7.0	6.9	6.9
Asx[a]	5	4.9	5.0	5.1	5.0
Glx[a]	1	1.1	1.2	1.1	1.2
Gly	1	1.0	1.1	1.0	1.2
His	1	1.2	1.3	1.1	1.2
Ile	1	1.1	1.0	1.0	1.0
Leu	4	4.0	4.1	4.2	4.1
Phe	1	1.1	1.0	1.0	1.0
Ser	2	1.9	1.9	1.8	2.0
Thr	2	2.1	2.0	2.0	2.0
Tyr	2	2.0	2.0	2.1	2.0
Val	2	2.0	2.0	1.9	2.1

[a] Asx: Asn and Asp; Glx: Gln and Glu.

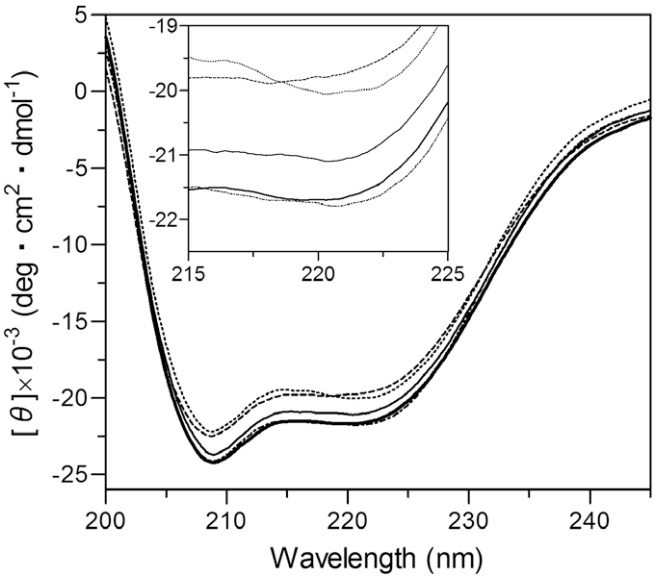

Fig. 2. CD spectra of synthetic VIP and derivatives. The measurements were carried out in 50% methanol/20 mM Tris–HCl buffer (pH 7.4). —, VIP; —, IK312532; - - - - -, IK312548; ·····, IK312550; -·- ·-, IK312551.

3.3. Solution-state stability data on novel VIP derivatives

Solution-state stability studies on novel VIP derivatives were carried out to assess the influence of chemical modification of IK31532 on its stability. Fig. 3A shows a semilogarithmic plot of potency (% remaining) of novel VIP derivatives versus time in sodium phosphate buffer at 40 °C. A linear relationship was obtained according to the following equation: $\ln A = \ln A_0 - kt$, (apparent first-order kinetics; $r = 0.972$), where A is the remaining peak area of VIP derivative, k is slope, and t is time (days). Stability of each peptide was evaluated on the basis of the kinetic degradation constant k with respect to the initial drug concentration, and the following data were obtained: slope (rate constant) = 0.21 day^{-1} for IK312532, 1.1×10^{-2} day^{-1} for IK312548, 1.8×10^{-2} day^{-1} for IK312550, and 1.1×10^{-2} day^{-1} for IK312551. Thus, IK312532, dissolved in sodium phosphate buffer (pH 7.4), exhibited the rapid degradation at 40 °C; however, the stability of three novel derivatives seemed to be improved significantly.

The Arrhenius plot was constructed from these observed first-order degradation rate constants at three temperatures (Fig. 3B). The plot shows a good linear relationship between logarithmic degradation rate (k) and the reciprocal of absolute temperature (T): $r = 0.998$ for IK312532, 0.988 for IK312548, 0.996 for IK312550, and 0.996 for IK312551 (Table 3). Activation energy (Ea) was calculated according to Arrhenius equation: $\ln k = \ln A - (Ea/RT)$, where A is the frequency factor, and R is the gas constant. Activation energy of IK312532 was calculated to be 20.2 kcal/mol, and it was close to the activation energy of adrenocorticotropic hormone fragment, showing deamination of asparaginyl residues as well [29]. There appeared to be significant differences in the frequency factor among VIP derivatives tested, and the chemical modification of IK312532 could lead to 10^5-fold reduction of frequency factor. From the Arrhenius parameters, stability of each peptide was predicted at 25 °C (Table 3), and the half-lives of novel derivatives, especially IK312551, were found to be 5–8-fold longer than that of IK312532. These observations suggested that substitution of amino acid residues at positions 24 and 25 resulted in the marked stabilization of VIP derivative.

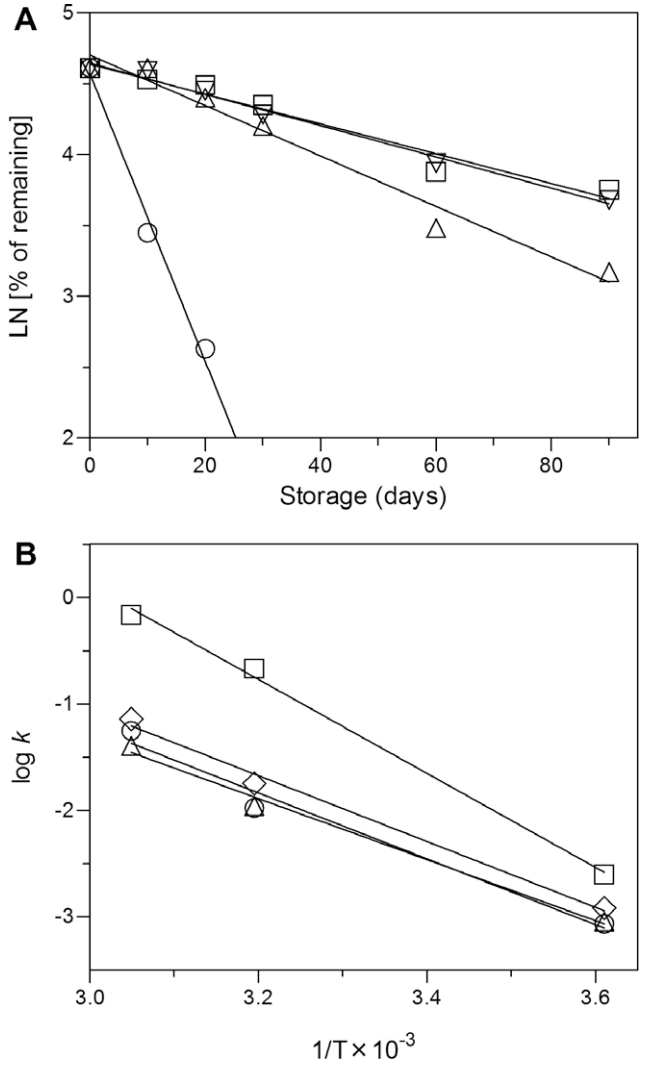

Fig. 3. Solution-state stability of VIP derivatives. (A) Time-dependent degradation of VIP derivatives. Each peptide (0.1 mg/mL) was dissolved in 20 mM sodium phosphate buffer (pH 7.4) and stored at 40 °C for indicated periods. ○, IK312532; □, IK312548; △, IK312550; and ▽, IK312551. Data represent mean of three experiments. (B) Arrhenius plotting for VIP derivatives. The logarithm of the degradation rate constant (k) is plotted vs $1000*(1/T)$, where T is the absolute temperature (K). ○, IK312532; □, IK312548; △, IK312550; and ▽, IK312551.

Table 3
Arrhenius parameters and prediction of stability of VIP derivative.

	Arrhenius parameters			Calculated values at 25 °C	
	Ea (kcal/mol)	A (day^{-1})	r	k (day^{-1})	$t_{0.5}$ (days)
IK312532	20.2	2.40×10^{13}	0.998	3.5×10^{-2}	19.6
IK312548	14.2	1.17×10^{8}	0.988	4.7×10^{-3}	146.8
IK312550	14.2	1.70×10^{8}	0.996	6.9×10^{-3}	100.2
IK312551	13.1	1.97×10^{7}	0.996	4.6×10^{-3}	151.1

Each parameter was calculated by computer fitting.

3.4. Biological activities of novel VIP derivatives

It is well established that VPAC2 receptor, a VIP-preferring receptor, is expressed in the alveolar wall [26], and our previous RT-PCR experiments revealed the dominant expression of the VPAC2 receptor in rat alveolar L2 cells [13]. In the present investigation, the binding activities of VIP and its derivatives for VPAC2

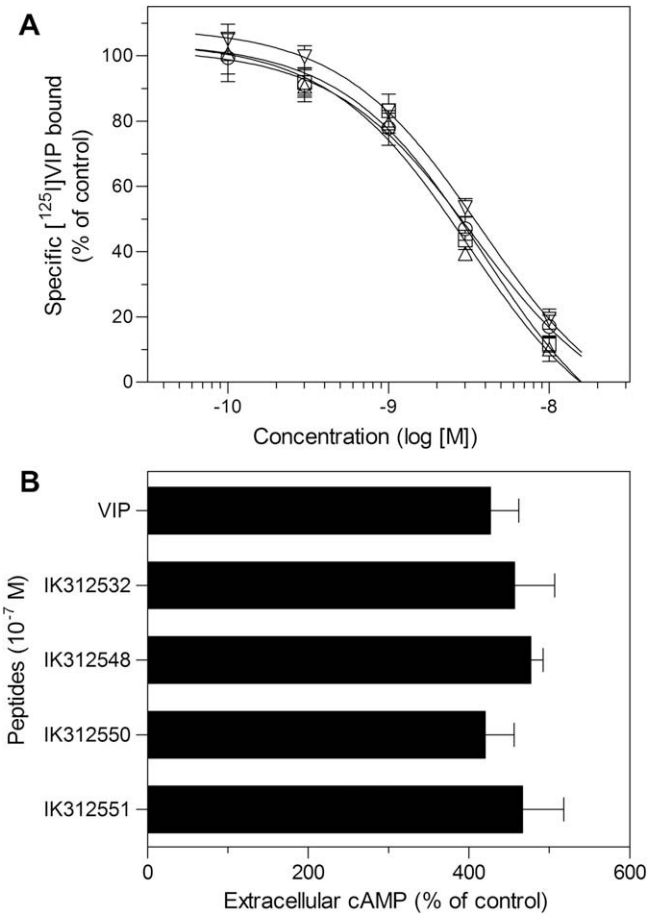

Fig. 4. *In vitro* pharmacology of VIP derivatives. (A) VIP receptor-binding activity in L2 cells. Concentration–inhibition curves for the effect of VIP on specific [^{125}I]VIP binding in L2 cells. Specific [^{125}I]VIP binding was measured in the absence and presence of increasing concentrations (10^{-10}–10^{-8} M) of VIP. ○, IK312532; □, IK312548; △, IK312550; and ▽, IK312551. (B) Stimulation of adenylate cyclase activation in L2 cells. L2 cells were stimulated with each peptide at the concentration of 10^{-7} M, and the amount of cAMP released was measured with an enzyme immunoassay. Each point represents a percentage (means ± SD, $n = 4$) of the control value.

receptor were examined with a radioligand binding assay using [^{125}I]VIP. Rosenthal analysis of the specific binding of [^{125}I]VIP (0.03–1.50 nM) in L2 cell membranes indicated a linear plot, and Kd and Bmax were estimated to $0.77 \pm 0.11 \times 10^{-9}$ M and $725 \pm 119 \times 10^{-15}$ mol/mg protein (mean ± SE, $n = 4$), respectively. As shown in Fig. 4A, VIP derivatives (each 10^{-10}–10^{-8} M) concentration dependently competed with [^{125}I]VIP for the binding sites in L2 cell membranes, and their inhibitory effects were nearly equipotent as shown by Ki values of $2.7 \pm 0.6 \times 10^{-9}$ (IK312532), $3.1 \pm 0.4 \times 10^{-9}$ (IK312548), $2.4 \pm 0.4 \times 10^{-9}$ (IK312550), and $3.1 \pm 0.5 \times 10^{-9}$ (IK312551) M. Our previous work revealed that VIP could compete with [^{125}I]VIP for VPAC2 receptor in rat lung with Ki value of $2.6 \pm 0.9 \times 10^{-9}$ M [12], being so similar to the binding activities of VIP derivatives tested. In addition, VIP derivatives at the concentration of 10^{-7} M caused a significant accumulation of cAMP in L2 cells, and their effects were found to be equipotent (Fig. 4B). These data suggest that novel VIP derivatives retain its biological activities despite the chemical modification of IK312532 at positions 8, 24, 25, and 28. This could be consistent with the observation in structural elucidation of VIP and its derivatives determined by CD spectral analysis.

Thus, the novel VIP derivatives were found to be equipotent with VIP or IK312532 in the receptor-binding activity and activation of adenylate cyclase. Next, the duration of action was assessed on the basis of neurite outgrowth in rat pheochromocytoma PC12 cells, where VPAC2 receptor, as well as PACAP-preferring (PAC1) and glucagon receptors, was expressing as determined by RT-PCR experiments (Fig. 5). It was well established that VIP exerted their biological functions in the central and peripheral nervous systems via the stimulation of various protein kinases including the phospholipase C/PKC and the mitogen-activated protein (MAP) kinase pathways, as well as the adenylate cyclase/PKA pathway [30,31].

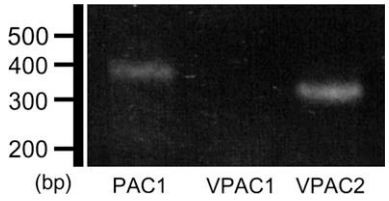

Fig. 5. RT-PCR analysis of PACAP/VIP receptor mRNAs in rat pheochromocytome PC12 cells. Total RNA was reverse transcribed in the presence of reverse transcriptase and PCR amplified with primer pairs specific for the PAC1, VPAC1, and VPAC2 receptors. Ethidium bromide-stained 2% agarose gels are shown. The data shown are representative of three experiments.

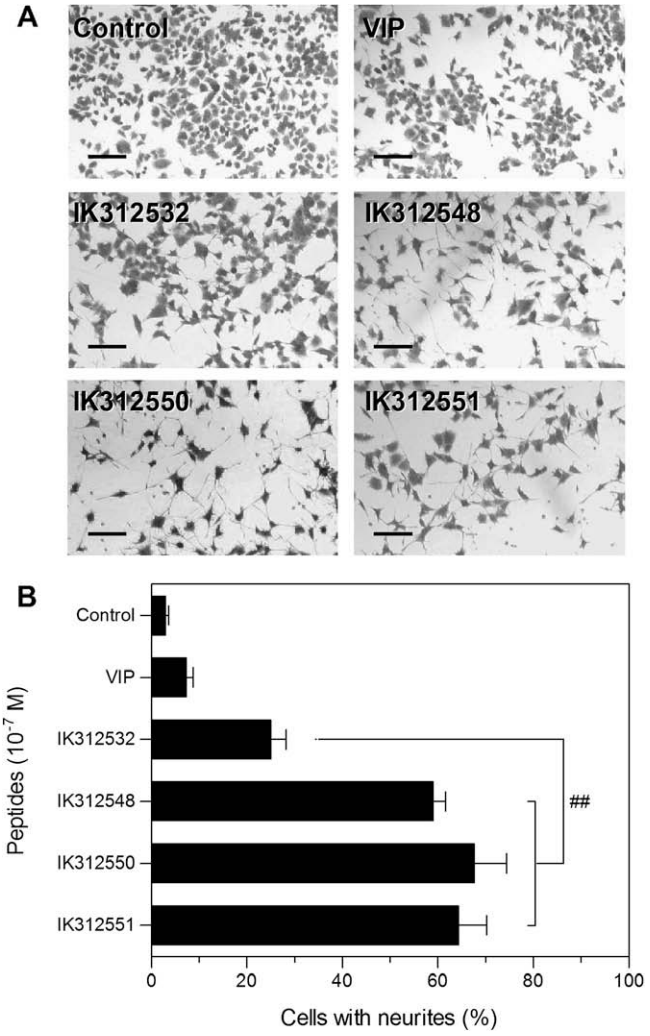

Fig. 6. Neurite outgrowth of PC12 cells stimulated by VIP and its derivatives. (A) Microscopic images from PC12 cells treated with VIPs at the concentration of 10^{-7} M for 72 h. Bar represents 100 μm. (B) VIPs-evoked stimulation of neurite outgrowth in PC12 cells. The percentage of cells with neuritis longer than 50 μm is shown. Each point represents a means ± SE of four experiments. ##, $P < 0.01$ between indicated groups.

In addition, sustained MAP kinase activation and cAMP appear to generate a signal for differentiation and neurite outgrowth in PC12 cells [32]. In this investigation, VIP at the concentration of 10^{-7} M stimulated differentiation of PC12 cells as evidenced by the slight promotion of neurite outgrowth (Fig. 6). All VIP derivatives tested exhibited significant enhancement of differentiation, particularly the addition of three novel VIP derivatives into PC12 cells culture resulted in more potent neurite outgrowth when compared to IK312532. The enhancement of neuromodulatory effect of VIP derivatives could be partly attributed to a higher chemical stability. Based on these pharmacological characterization of VIP derivatives, taken together with the stability data, [$A^{8,24,25}$, $R^{15,20,21}$, L^{17}, des-N^{28}]-VIP-GRR (IK312551) could be a potent lead compound for promising therapeutic agents.

4. Conclusions

In the present investigation, we demonstrated that IK312532, a long-lasting VIP derivative, was susceptible to degradation in solution state, producing mainly three degradants with similar amino acid composition. Chemical modification of VIP derivative, particularly amino acid at position 24, led to the significant improvement in chemical stability. Newly synthesized VIP derivatives exhibited similar receptor-binding activity and stimulation of adenylate cyclase when compared to VIP and IK312532, whereas neurotrophic action of novel VIP derivatives in PC12 cells was found to be far higher. Upon these findings, deamination of Asn residue at position 24, by direct hydrolysis or via acyclic imide intermediate, is likely to responsible for degradation of IK312532. The stabilization of VIP derivative by chemical modification at position 24 could lead to the enhanced neurite outgrowth of PC12 cells, possibly due to extended duration of action.

Acknowledgements

We wish to thank Kosuke Endo, Pharmaceutical Division, Ito Life Sciences Inc., for his excellent technical assistance throughout this work. This work was supported in part by a Grant-in-aid for Young Scientists (B) (No. 20790103; S. Onoue) from the Ministry of Education, Culture, Sports, Science and Technology.

References

[1] S.I. Said, V. Mutt, Polypeptide with broad biological activity: isolation from the small intestine, Science 169 (1970) 1217–1218.
[2] R.H. Unger, R.E. Dobbs, L. Orci, Insulin, glucagon, and somatostatin secretion in the regulation of metabolism, Annu. Rev. Physiol. 40 (1978) 307–343.
[3] D. Vaudry, B.J. Gonzalez, M. Basille, L. Yon, A. Fournier, H. Vaudry, Pituitary adenylate cyclase-activating polypeptide and its receptors: from structure to functions, Pharmacol. Rev. 52 (2000) 269–324.
[4] S.I. Said, Vasoactive intestinal polypeptide (VIP) in asthma, Ann. NY Acad. Sci. 629 (1991) 305–318.
[5] S. Onoue, Y. Waki, K. Hamanaka, Y. Takehiko, K. Kashimoto, Vasoactive intestinal peptide regulates catecholamine secretion in rat PC12 cells through the pituitary adenylate cyclase activating polypeptide receptor, Biomed. Res. 22 (2001) 77–82.
[6] M. Delgado, C. Martinez, D. Pozo, J.R. Calvo, J. Leceta, D. Ganea, R.P. Gomariz, Vasoactive intestinal peptide (VIP) and pituitary adenylate cyclase-activation polypeptide (PACAP) protect mice from lethal endotoxemia through the inhibition of TNF-alpha and IL-6, J. Immunol. 162 (1999) 1200–1205.
[7] N. Inagaki, H. Kuromi, S. Seino, PACAP/VIP receptors in pancreatic beta-cells: their roles in insulin secretion, Ann. NY Acad. Sci. 805 (1996) 44–51.
[8] M. Shirai, A. Maki, M. Takanami, K. Ando, K. Nakamura, N. Yanaihara, C. Yanaihara, K. Iguchi, T. Fujita, T. Iwanaga, Content and distribution of vasoactive intestinal polypeptide (VIP) in cavernous tissue of human penis, Urology 35 (1990) 360–363.
[9] M. Delgado, C. Abad, C. Martinez, J. Leceta, R.P. Gomariz, Vasoactive intestinal peptide prevents experimental arthritis by downregulating both autoimmune and inflammatory components of the disease, Nat. Med. 7 (2001) 563–568.
[10] S. Onoue, S. Misaka, S. Yamada, Structure–activity relationship of vasoactive intestinal peptide (VIP): potent agonists and potential clinical applications, Naunyn Schmiedebergs Arch. Pharmacol. 377 (2008) 579–590.
[11] S. Onoue, S. Yamada, T. Yajima, Bioactive analogues and drug delivery systems of vasoactive intestinal peptide (VIP) for the treatment of asthma/COPD, Peptides 28 (2007) 1640–1650.
[12] S. Onoue, Y. Ohmori, A. Matsumoto, S. Yamada, R. Kimura, T. Yajima, K. Kashimoto, Structure–activity relationship of synthetic truncated analogues of vasoactive intestinal peptide (VIP): an enhancement in the activity by a substitution with arginine, Life Sci. 74 (2004) 1465–1477.
[13] S. Onoue, Y. Ohmori, K. Endo, S. Yamada, R. Kimura, T. Yajima, Vasoactive intestinal peptide and pituitary adenylate cyclase-activating polypeptide attenuate the cigarette smoke extract-induced apoptotic death of rat alveolar L2 cells, Eur. J. Biochem. 271 (2004) 1757–1767.
[14] Y. Ohmori, S. Maruyama, R. Kimura, S. Onoue, A. Matsumoto, K. Endo, T. Iwanaga, K. Kashimoto, S. Yamada, Pharmacological effects and lung-binding characteristics of a novel VIP analogue, [R15, 20, 21, L17]-VIP-GRR (IK312532), Regul. Pept. 123 (2004) 201–207.
[15] R.B. Merrifield, Solid-phase peptide synthesis, Adv. Enzymol. Relat. Areas Mol. Biol. 32 (1969) 221–296.
[16] Y.H. Chen, J.T. Yang, H.M. Martinez, Determination of the secondary structures of proteins by circular dichroism and optical rotatory dispersion, Biochemistry 11 (1972) 4120–4131.
[17] N. Greenfield, G.D. Fasman, Computed circular dichroism spectra for the evaluation of protein conformation, Biochemistry 8 (1969) 4108–4116.
[18] M.A. Andrade, P. Chacon, J.J. Merelo, F. Moran, Evaluation of secondary structure of proteins from UV circular dichroism spectra using an unsupervised learning neural network, Protein Eng. 6 (1993) 383–390.
[19] W.H.J. Douglas, M.E. Kaighn, Clonal isolation of differentiated rat lung cells, In Vitro 10 (1974) 230–237.
[20] P. Leroux, H. Vaudry, A. Fournier, S. St-Pierre, G. Pelletier, Characterization and localization of vasoactive intestinal peptide receptors in the rat lung, Endocrinology 114 (1984) 1506–1512.
[21] O.H. Lowry, N.J. Rosebrough, A.L. Farr, R.J. Randall, Protein measurement with the folin phenol reagent, J. Biol. Chem. 193 (1951) 265–275.
[22] S. Capasso, L. Mazzarella, F. Sica, A. Zagari, Deamination via cyclic imide in asparaginyl peptides, Pept. Res. 2 (1989) 195–200.
[23] R. Tyler-Cross, V. Schirch, Effect of amino acid sequence, buffers, and isonic strength on the rate and mechanism of deamination of asparagine residues in small peptides, J. Biol. Chem. 266 (1991) 22549–22556.
[24] M. Bodanszky, A. Bodanszky, Y.S. Klausner, S.I. Said, A preferred conformation in the vasoactive intestinal peptide (VIP), molecular architecture of gastrointestinal hormones, Bioorg. Chem. 3 (1974) 133–140.
[25] M. Bodanszky, A. Bodanszky, Conformation of peptides of the secretin-VIP-glucagon family in solution, Peptides 7 (1986) 43–48.
[26] R.M. Robinson, E.W. Blakeney Jr., W.L. Mattice, Lipid-induced conformational changes in glucagon, secretin, and vasoactive intestinal peptide, Biopolymers 21 (1982) 1228–1271.
[27] S. Onoue, A. Matsumoto, Y. Nagano, K. Ohshima, Y. Ohmori, S. Yamada, R. Kimura, T. Yajima, K. Kashimoto, Alpha-helical structure in the C-terminus of vasoactive intestinal peptide: functional and structural consequences, Eur. J. Pharmacol. 485 (2004) 307–316.
[28] M. O'Donnell, R.J. Garippa, N.C. O'Neill, D.R. Bolin, J.M. Cottrell, Structure–activity studies of vasoactive intestinal polypeptide, J. Biol. Chem. 266 (1991) 6389–6392.
[29] K. Patel, R.T. Borchardt, Chemical pathways of peptide degradation. II. Kinetics of deamidation of an asparaginyl residue in a model hexapeptide, Pharm. Res. 7 (1990) 703–711.
[30] D. Vaudry, C. Rousselle, M. Basille, A. Falluel-Morel, T.F. Pamantung, M. Fontaine, A. Fournier, H. Vaudry, B.J. Gonzalez, Pituitary adenylate cyclase-activating polypeptide protects rat cerebellar granule neurons against ethanol-induced apoptotic cell death, Proc. Natl. Acad. Sci. USA 99 (2002) 6398–6403.
[31] D. Vaudry, B.J. Gonzalez, M. Basille, T.F. Pamantung, M. Fontaine, A. Fournier, H. Vaudry, The neuroprotective effect of pituitary adenylate cyclase-activating polypeptide on cerebellar granule cells is mediated through inhibition of the CED3-related cysteine protease caspase-3/CPP32, Proc. Natl. Acad. Sci. USA 97 (2000) 13390–13395.
[32] H.S. Kim, S. Yumkham, S.H. Kim, K. Yea, Y.C. Shin, S.H. Ryu, P.G. Suh, Secretin induces neurite outgrowth of PC12 through cAMP-mitogen-activated protein kinase pathway, Exp. Mol. Med. 38 (2006) 85–93.